Supplementary Figures

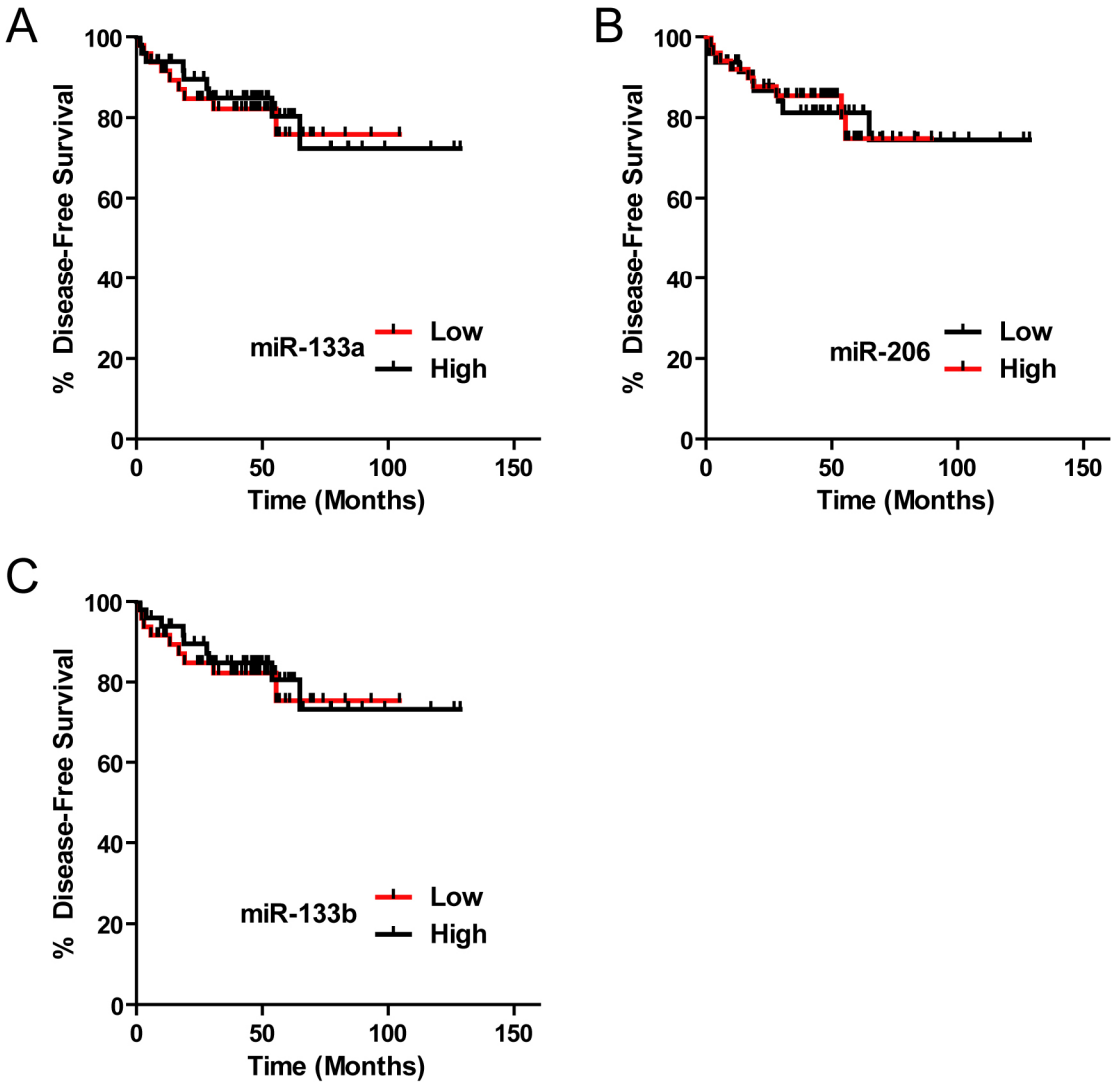

Supplementary Figure 1. Kaplan-Meier analysis of disease recurrence. Neither expression of miR-133a (A), miR-206 (B), nor miR-133b (C) was significantly associated with disease recurrence. Median expression of miRs in primary prostate tumors was used as the cutoff**.** High versus low miR expression was compared in the recurrence analysis.

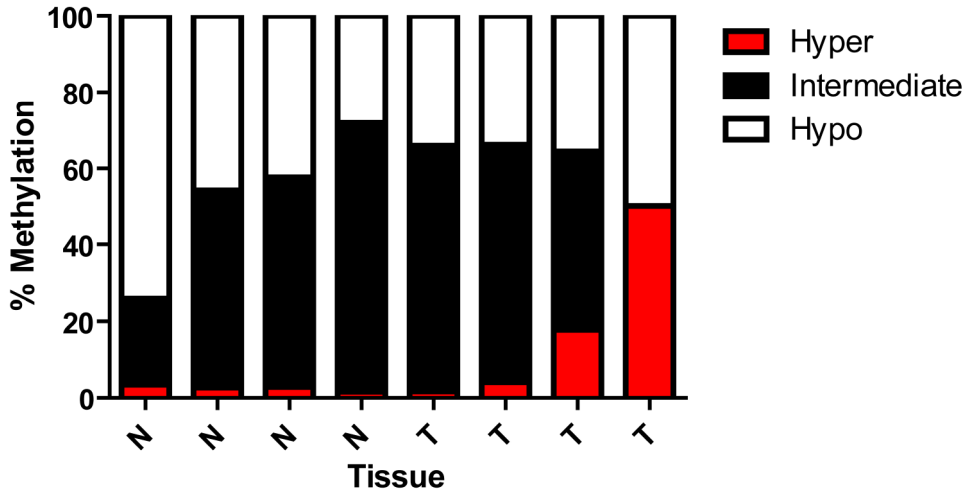

Supplementary Figure 2. miR-1(-1) CpG island methylation status in prostate tissues from prostate cancer patients. Adjacent non-cancerous (N) and tumor (T) tissues were assessed for percent hypo-, intermediate, and hyper-methylation of the CpG island-81 upstream of the miR-1-1 gene (see also Figure 1A). Methylation status was assessed with the EpiTect Methyl qRCP primer assay, as described in supplementrary methods, and average C_T values were used to calculate the fraction of hypermethylated (F_{HM}), unmethylated (F_{UM}) and intermediately methylated (F_{IM}) DNA using the equations; $F_{HM}=(2^{-Ct(\mathrm{Ms})}/(2^{-Ct(\mathrm{Mo})}- 2^{-Ct(\mathrm{Msd})}))$, $F_{UM}=(2^{-Ct(\mathrm{Md})}/(2^{-Ct(\mathrm{Mo})}- 2^{-Ct(\mathrm{Msd})}))$, and $F_{IM}= 1-F_{HM}-F_{UM}$. A tissue is considered hypermethylation-positive when hypermethylation by this assay reaches 10% to 20% (EpiTect Methyl qPCR Assay handbook).

A

miRNA	Cell Line	Avg *Ct*	SD *Ct*	Δ*Ct*	SD Δ*Ct*	miRNA Expression
miR-1	RWPE-1	38.5	2.5	8.7	0.2	0.002
	22Rv1	38.8	2.1	9.1	0.2	0.002
	LNCaP	39	1.8	9.6	0.3	0.001
miR-206	RWPE-1	36.8	3.1	6.9	0.1	0.008
	22Rv1	35.1	1.4	5.4	0.2	0.023
	LNCaP	37.2	2.5	7.8	0.1	0.005
miR-27	RWPE-1	22.8	0.2	-7.1	0.9	135.14
	22Rv1	24.4	0.6	-5.3	0.2	38.816
	LNCaP	26.7	0.3	-2.7	0.1	6.665

B

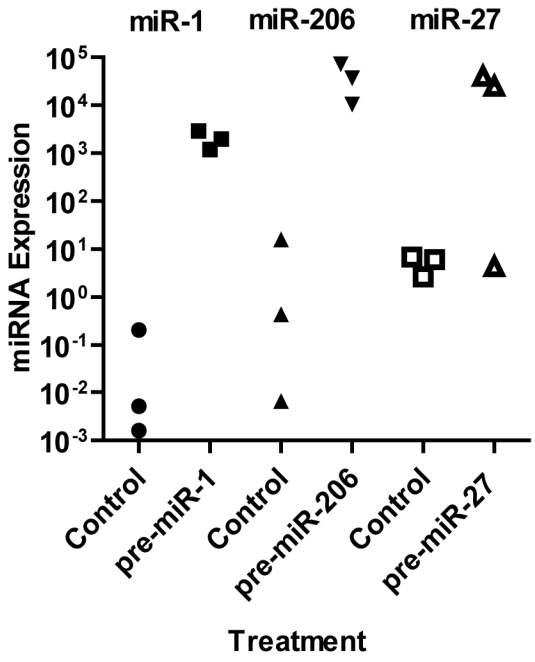

Supplementary Figure 3. Endogenous and ectopic expression of miR-1, miR-206, and miR-27 in prostate cancer cells. (A) Baseline miRNA expression was estimated using stem-loop real-time PCR in RWPE-1, 22Rv1, and LNCaP cells. Both miR-1 and miR-206 expression levels were near the detection limit of the assay. Average (Avg) *Ct*, standard deviation (SD), Δ*Ct* normalized to U6, and relative expression ($2^{-\Delta Ct}$) are shown. **(B)** LNCaP cells were transfected with 30 nM pre-miR oligos for miR-1, miR-206, and miR-27, or scrambled control pre-miR oligos. Forty-eight hours post transfection, a stem loop real-time PCR was performed to assess up-regulation of the transfected miRs. Shown is the relative miR abundance for three independent experiments, assayed in triplicate and expressed as $2^{-\Delta Ct}$.

A

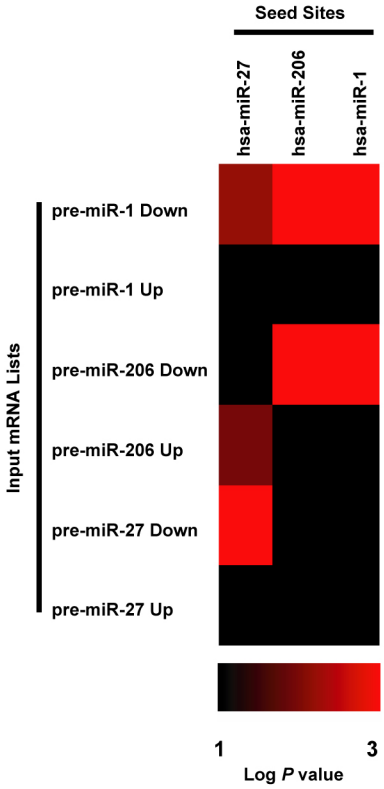

B

	miR-1		miR-206		
Gene ID	Fold Change	*P* value	Fold Change	*P* value	Gene Description
LASP1	-3.88	1.65E-04	-4.04	2.19E-04	LIM and SH3 protein 1
SERP1	-3.01	5.13E-04	-3.86	6.05E-05	stress-associated endoplasmic reticulum protein 1
MMD	-2.98	1.83E-04	-3.25	1.56E-04	monocyte to macrophage differentiation-associated
TWF1	-2.75	5.74E-04	-4.45	1.47E-03	twinfilin, actin-binding protein, homolog 1 (Drosophila)
TAGLN2	-2.73	4.56E-03	-3.29	2.05E-03	transgelin 2
PTMA	-2.43	1.03E-03	-2.79	2.21E-04	prothymosin, alpha
RNF38	-2.36	6.03E-05	-2.57	4.15E-05	ring finger protein 38
SFRS9	-2.33	6.16E-05	-3.01	7.13E-06	splicing factor, arginine/serine-rich 9
MGC5139	-2.27	1.87E-04	-2.93	2.26E-05	hypothetical protein MGC5139
G6PD	-2.19	3.77E-03	-3.03	3.93E-04	glucose-6-phosphate dehydrogenase
POGK	-2.17	2.27E-03	-3.17	1.29E-04	pogo transposable element with KRAB domain
TMCC1	-2.14	2.75E-04	-2.12	9.00E-04	transmembrane and coiled-coil domain family 1
EFNB2	-1.99	2.55E-03	-2.28	1.01E-03	ephrin-B2
KIF2A	-1.92	1.49E-03	-2.10	8.42E-04	kinesin heavy chain member 2A
NUP50	-1.92	3.44E-04	-1.93	5.24E-04	nucleoporin 50kDa
ARHGEF18	-1.90	1.16E-04	-2.31	1.44E-05	rho/rac guanine nucleotide exchange factor (GEF) 18
CAP1	-1.89	1.42E-03	-2.69	1.75E-05	CAP, adenylate cyclase-associated protein 1 (yeast)
SLC25A1	-1.87	1.05E-02	-3.14	1.67E-04	solute carrier family 25 member 1
TSPAN4	-1.80	6.17E-03	-1.51	1.11E-03	tetraspanin 4
ADAR	-1.77	9.79E-04	-1.71	2.48E-03	adenosine deaminase, RNA-specific
RNF138	-1.76	3.59E-03	-2.20	4.31E-04	ring finger protein 138
H3F3B	-1.76	2.80E-04	-1.75	4.94E-04	H3 histone, family 3B (H3.3B)
HMGN1	-1.68	5.75E-04	-1.96	9.36E-05	high-mobility group nucleosome binding domain 1
HNRPU	-1.68	1.15E-02	-1.57	3.16E-02	heterogeneous nuclear ribonucleoprotein U
SNX2	-1.66	4.92E-03	-1.70	5.42E-03	sorting nexin 2
DHX15	-1.65	5.52E-03	-1.77	3.43E-03	DEAH (Asp-Glu-Ala-His) box polypeptide 15
PTBP1	-1.65	3.52E-03	-2.06	7.44E-05	polypyrimidine tract binding protein 1
DIMT1L	-1.64	6.00E-03	-2.07	5.06E-04	DIM1 dimethyladenosine transferase 1-like
TDG	-1.63	1.88E-03	-1.61	3.60E-03	thymine-DNA glycosylase
ARF4	-1.63	3.83E-03	-2.11	1.87E-04	ADP-ribosylation factor 4
MEA1	-1.62	2.04E-03	-2.22	3.81E-05	male-enhanced antigen 1
BLCAP	-1.60	1.09E-05	-1.69	6.74E-06	bladder cancer associated protein
PICALM	-1.60	2.74E-03	-2.32	1.64E-02	phosphatidylinositol binding clathrin assembly protein
GAS2L1	-1.56	9.20E-03	-1.57	4.47E-03	growth arrest-specific 2 like 1
ATP6V1A	-1.54	7.31E-03	-2.26	1.16E-02	ATPase, H+ transporting, lysosomal 70kDa, V1 subunit A
TNKS2	-1.52	3.48E-04	-1.70	6.16E-05	tankyrase-2

Supplementary Figure 4. Down-regulated transcripts in pre-miR-1/206 transfected LNCaP cells are enriched for miR-1/206 3'UTR seed sites. (A) MiR target enrichment ("seed sites") is shown for both down-regulated ("down") and up-regulated ("up") transcripts after transfection of LNCaP cells with pre-miRs. Expression of scrambled miR is the baseline control. There was enrichment for predicted miR-1/206 targets only among the down-regulated genes, as shown by the red color. TargetScan was used to define miR target genes. MiR-27 target enrichment results are shown for comparison. The color coding of the heatmap is expressed as the −Log(*P* value)-based enrichment of computationally predicted 3'UTR target sites for the corresponding pre-miR transfection and the down-/up-regulated transcripts. Red color indicates enrichment along the log *P* value scale. Black indicates no enrichment. Lists were generated using cutoffs for FDR ≤0.3% and ≥1.5-fold decrease. (B) Genes down-regulated by both miR-1 and miR-206 in LNCaP cells. MiR-1 and miR-206 regulate the abundance of many of the same transcripts. Table shows down-regulated transcripts with miR-1/206 seed sites after transfection of LNCaP cells with pre-miR oligos.

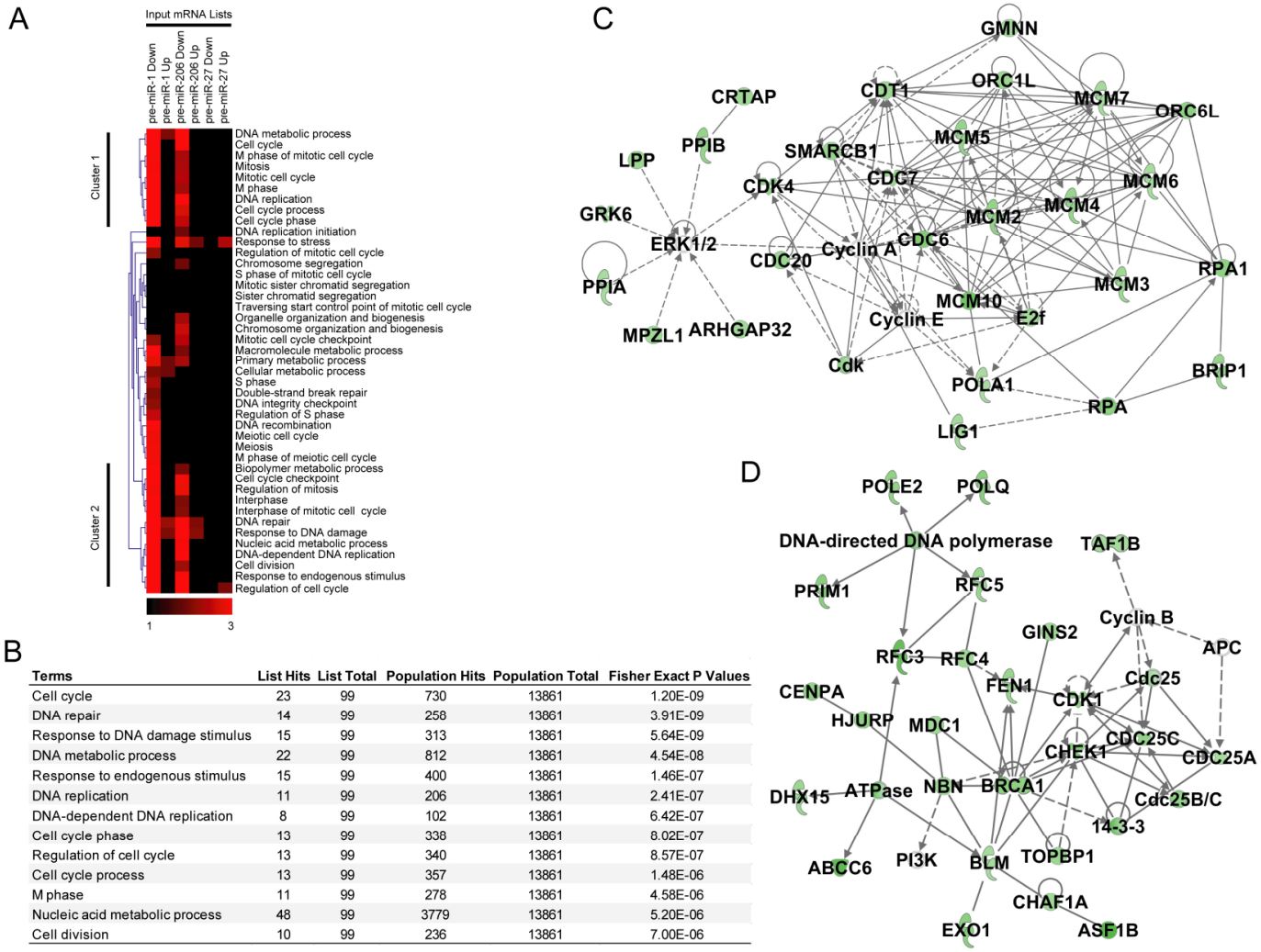

B

Terms	List Hits	List Total	Population Hits	Population Total	Fisher Exact P Values
Cell cycle	23	99	730	13861	1.20E-09
DNA repair	14	99	258	13861	3.91E-09
Response to DNA damage stimulus	15	99	313	13861	5.64E-09
DNA metabolic process	22	99	812	13861	4.54E-08
Response to endogenous stimulus	15	99	400	13861	1.46E-07
DNA replication	11	99	206	13861	2.41E-07
DNA-dependent DNA replication	8	99	102	13861	6.42E-07
Cell cycle phase	13	99	338	13861	8.02E-07
Regulation of cell cycle	13	99	340	13861	8.57E-07
Cell cycle process	13	99	357	13861	1.48E-06
M phase	11	99	278	13861	4.58E-06
Nucleic acid metabolic process	48	99	3779	13861	5.20E-06
Cell division	10	99	236	13861	7.00E-06

Supplementary Figure 5. MiR-1/206 down-regulated mRNAs are enriched for transcripts regulating cell cycle and DNA damage response. (A) GO biological processes (GOBP) enriched in down- or up-regulated transcripts after transfection of LNCaP cells with pre-miRs (cutoff $P < 0.01$). MiR-1/206 targeted biological processes are highlighted as clusters 1 and 2. Heat map shows enrichment (−Log(P value)-based) for biological processes within gene lists for both down-regulated ("down") and up-regulated ("up") transcripts. Red color intensity is a surrogate for the relative enrichment of differentially expressed genes in a biological process. (B) Ranking of GO biological processes by their enrichment score. Table shows the biological processes with the most significant transcript enrichment after miR-1 expression in LNCaP cells. Input list consisted of down-regulated genes at the $P < 0.01$ significance level. (C) Network of genes involved in cell cycle control that is targeted by miR-1. (D) Network of genes involved in the DNA damage response that is targeted by miR-1. Genes colored as green were down-regulated by miR-1/miR-206.

A

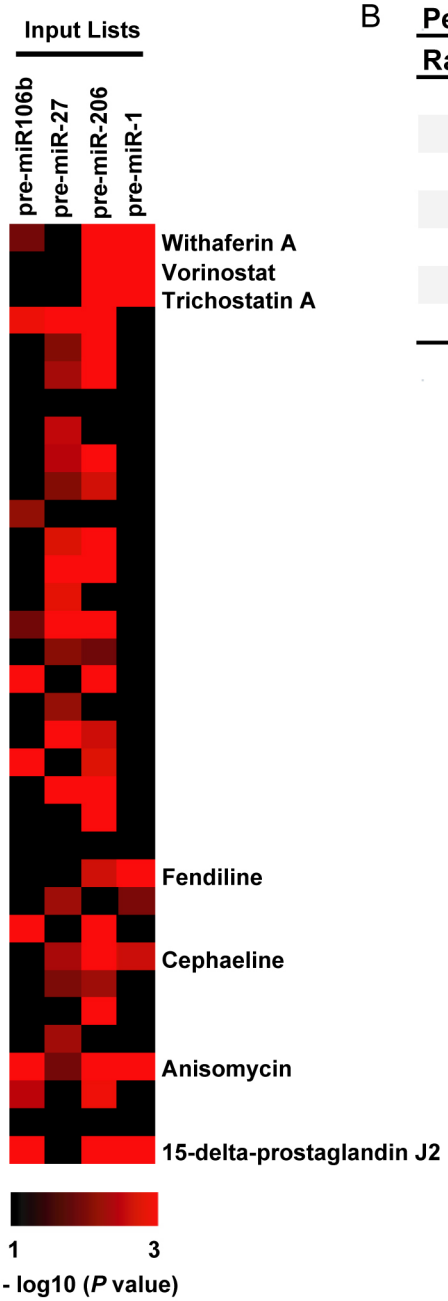

B

Perturbagens related to miR-1 expression patterns

Rank	cmap name	*P* value
1	vorinostat	<0.00004
2	trichostatin A	<0.00004
3	withaferin A	0.00004
4	15-delta prostaglandin J2	0.00006
5	fendiline	0.00012
6	anisomycin	0.00014
7	cephaeline	0.00338

Supplementary Figure 6. Connectivity mapping suggests that miR-1 expression and histone deacetylase inhibitor treatment induce similar phenotypes. (A) Shown is a heatmap highlighting significant relationships between miR-induced mRNA signatures in LNCaP cells and mRNA signatures induced by small molecule drugs across multiple human cancer cells. Functional connections between miR-1/206-induced signatures and signatures induced by small molecules (total 1309 molecules that target cancer and other diseases) were explored using the Connectivity Map database at http:// www.broad.mit.edu/cmap. There is significant overlap between the miR-1/206-induced signatures and gene signatures induced by withaferin A and the two histone deacetylase inhibitors, vorinstat and trichostatin A (Permutation *P* value <0.0001). Red indicates a significant relationship [- log10 (*P* value)-based]. Query gene signatures were generated with cutoffs for differentially expressed mRNAs at ≥ 1.5-fold decrease and FDR ≤ 0.3%. (B) Ranking of the small molecule-induced gene signatures based on their relationship with the miR-1-induced gene expression pattern.

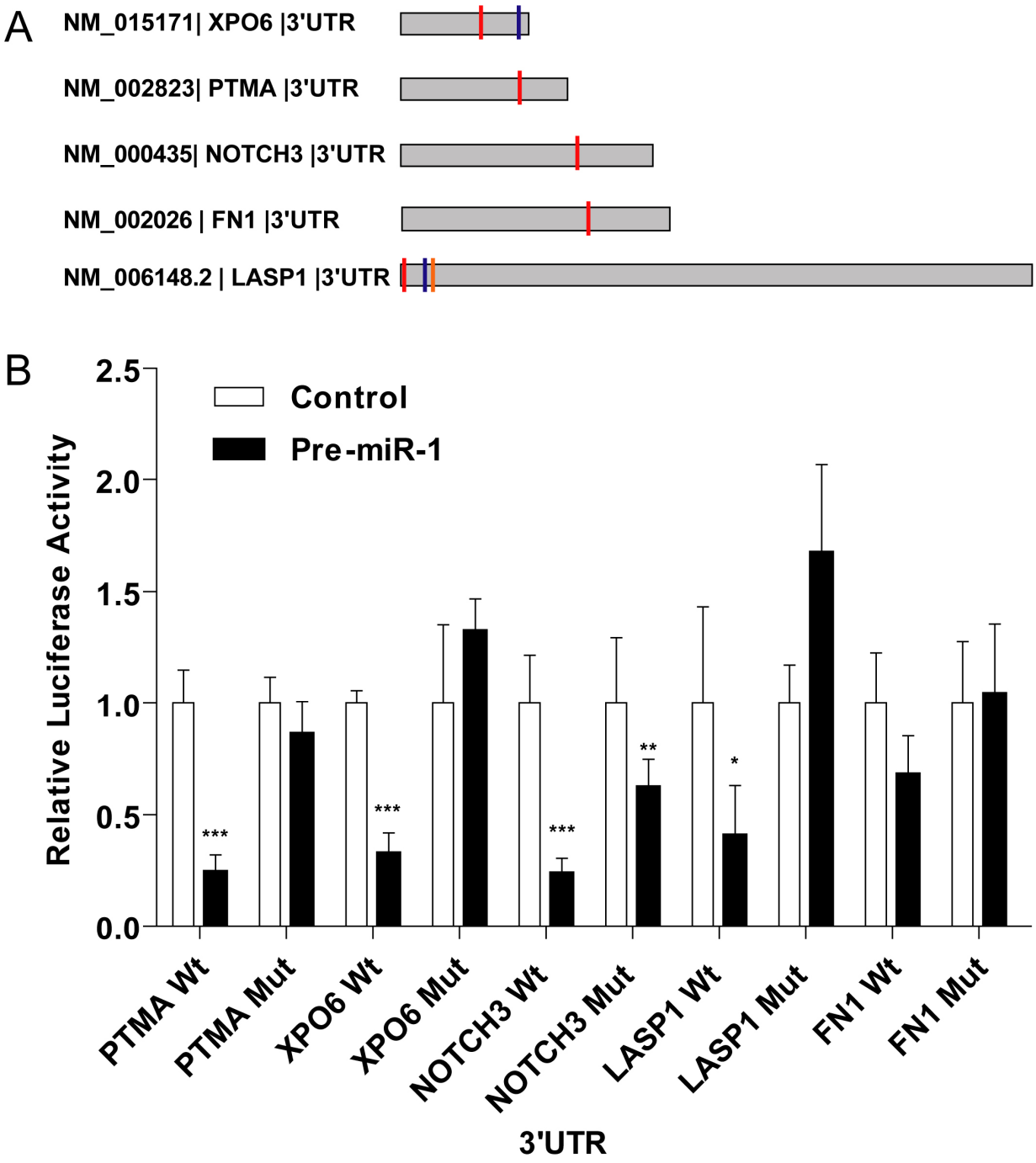

Supplementary Figure 7. 3'UTR reporter assays for miR-1 interference with translation. (A) Schematic - showing various 3'UTRs with the predicted miR-1 seed site locations for candidate miR-1 target transcripts. (B) 3'UTR reporter assays using wild-type and mutant 3'UTR luciferase reporter constructs. LNCaP cells were transfected with these constructs and pre-miR-1 or scrambled negative pre-miR control. Relative luciferase activity in cell extracts was determined 48 hrs post transfection. All values represent the average normalized luciferase activity of four replicates +/- standard deviation. Shown is one of three representative experiments. *P* values were calculated with the student t-test comparing pre-miR-1 transfected cells versus pre-miR negative control transfected cells. * $P < 0.05$, ** $P < 0.01$, *** $P < 0.001$.

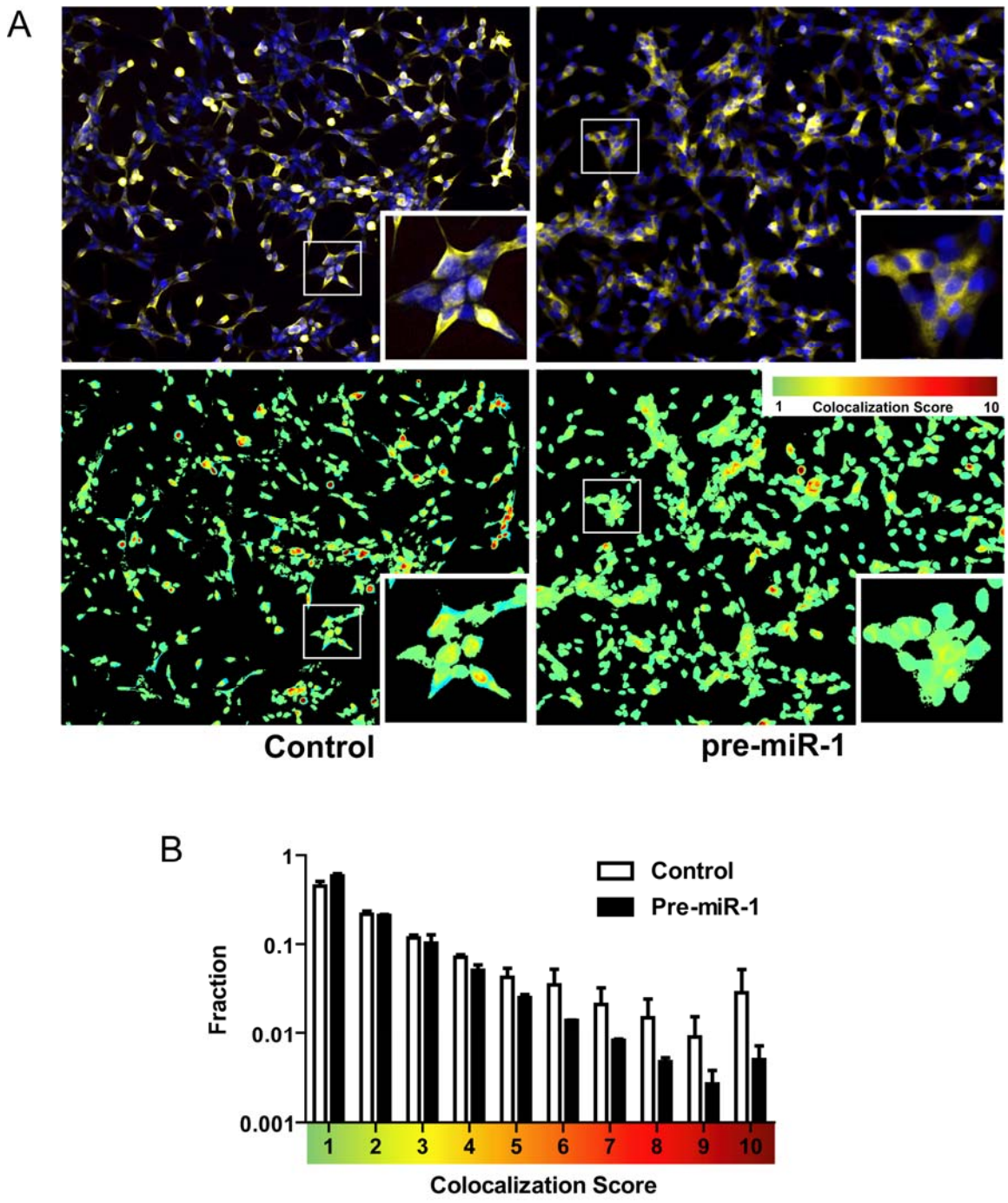

Supplementary Figure 8. Pre-miR-1 transfection of LNCaP alters intracellular LASP-1 localization. (A) LASP1 is less nuclear and more cytosolic in the pre-miR-1 transfected cells, as shown by the altered localization using a fluorescence-labeled anti-LASP1 antibody. Top panel shows DAPI (Blue) and LASP-1 (Yellow) staining in LNCaP cells transfected with control and pre-miR-1 oligos. Bottom panel shows images of representative quantification of DAPI and LASP-1 colocalization with yellow and red pseudo color indicating coloalization. Insets show higer magnification of LASP-1 and DAPI staining. (B) Colocalization scores of control and pre-miR-1 treated LNCaP cells shows shift in DAPI and LASP-1 colocaltization. Graph represents average of three fields per treatment +/- SD from one of three independent experiments.

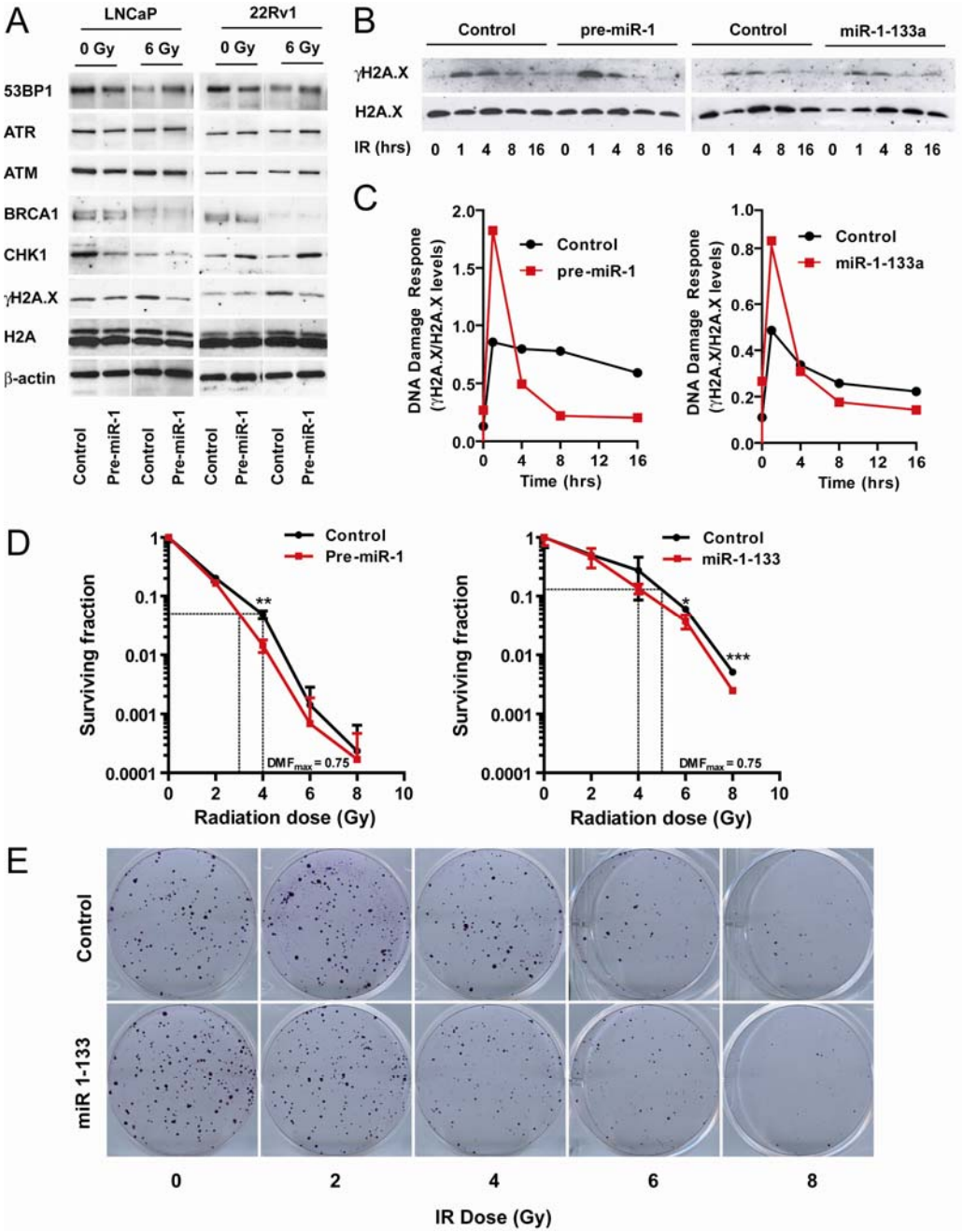

Supplementary Figure 9. DNA damage response to radiation in prostate cancer cells expressing miR-1 or the complete miR-1-133 cluster. (A) Expression of proteins involved in DNA damage response in LNCaP and 22Rv1 cells transfected with control or pre-miR-1 oligos (16 hours) and irradiated with and without 6 Gy radiation. Twenty-four hours post-irradiation, protein extracts were prepared and 25 μg of extract was loaded per lane. Loading controls: β-actin and total H2A histone. (B) Time course of histone 2A.X phosphorylation ("γH2A.X") and parent histone 2A.X protein levels in response to radiation (IR) in pre-miR-1 transfected (right) or miRNA-1-133 cluster expressing (left) 22Rv1 cells. (C) Graphs show densitometry measurements of the γH2A.X/H2A.X ratio for the time course experiment shown in B. (D) Log scale survival curves after irradiation of 22Rv1 cells. Cells were either transiently transfected with pre-miR-1 or control oligos (left), or infected with lentiviral constructs encoding the complete miRNA-1-133 cluster or only the reporter gene (vector control) (E) Representative images of the colony formation assay for control or miR-1-133 lentiviral infected 22Rv1 cells irradiated with various amounts of radiation. There was a statistically significant difference in the surviving fraction of cells between the pre-miR-1 or miR-1-133 cluster expressing cells and the control cells at various doses (* P = 0.02; ** 0.002; *** < 0.001), with pre-miR-1/miR-1-133 expressing cells showing decreased survival.

Supplementary Methods

DNA methylation analysis. Snap-frozen non-tumor and tumor prostate tissues from University of Maryland were embedded in OCT and cut at 5 microns. H and E staining and pathological examination for each tissue was performed to ensure tumor content. 3-4 slides from 4 tumors and 4 non-tumor tissue (unpaired) were used for DNA isolation using QIAamp DNA Micro Kit (Qiagen). The methylation status of the CpG island-81 (location; chr20:61832167-61833074) within the promoter of miR-1-1 was examined using EpiTect Methyl qRCP primer assay (Qiagen; MePH90226-1A) and EpitTect Methyl DNA restriction Kit, following the suppliers directions. To prepare DNA for real-time PCR analysis, 125 ng was separated into mock (Mo), methylation-sensitive (Ms), methylation-dependent (Md), and methylation-sensitive/dependent (Msd) enzyme digests. Real-time PCR was performed using 2 µL of each digest, 0.4 ul PCR primer mix, in a 10 ul PCR using RT^2 SYBR Green ROX qPCR Mastermix according to the manufacturer's instructions in a 384-well ABI 7900 system. Reactions were performed in triplicate and average C_T values were used to calculate the fraction of hypermethylated (F_{HM}), unmethylated (F_{UM}) and intermediately methylated (F_{IM}) DNA using the equations; $F_{HM}=(2^{-Ct(\mathrm{Ms})}/(2^{-Ct(\mathrm{Mo})}-2^{-Ct(\mathrm{Msd})}))$, $F_{UM}=(2^{-Ct(\mathrm{Md})}/(2^{-Ct(\mathrm{Mo})}-2^{-Ct(\mathrm{Msd})}))$, and $F_{IM}= 1-F_{HM}-F_{UM}$. A tissue is considered hypermethylation-positive when hypermethylation by this assay reaches 10%-20% (EpiTect Methyl qPCR Assay handbook).

Clonogenic assay. 22Rv1cells were seeded at 400, 800, 1600, 3200, and 6400 cells per 6-well. 24 hours post plating, cells were irradiated using a cesium-137 chamber at 1.6 Gy/min to achieve a dose of 0, 2, 4, 6, and 8. Two weeks later colonies were washed in PBS, fixed in 100% methanol for 10 minutes, stained with 0.5% crystal violet for 5 min and washed in PBS. Colonies of >50 cells were quantified using ImageJ software and surviving fraction was calculated using the formula: colonies counted/cells plated × plating efficiency, where plating efficiency is defined as mean colonies counted/cells plated for non-irradiated control. Experiments were conducted in triplicate and presented as means ± SD. Maximum Dose Modifying Factor (DMFmax) for pre-miR-1 or miR-1-133 cluster was calculated as dose to produce an effect with radioprotector/dose to produce the same effect without radioprotector. A ratio < 1 indicates a radioprotective effect.

LASP1 and F-actin fluorescence labeling and determination of mitotic index. Cells ($2.5x10^5$) were cultured on glass coverslips in six-well plates before being transfected with pre-miR oligos as described before. After treatment for 48 hr, coverslips were washed with PBS, fixed in 4% paraformaldehyde, and permeabilize with 0.1% Triton X-100 in PBS for 5 minutes. Cloverslips were then blocked in goat serum (BioGenex, San Ramon, CA) for 1 hr at room temperature (RT) before incubation with primary mouse LASP1 antibody 1:200 overnight at 4^oC. Cells were incubated in 1:200 secondary goat anti-mouse 488 antibody (Invitrogen) in PBS/0.1% Triton X-100 with F-actin stain (1 unit of phalloidin-568; Invitrogen) for 30 minutes at RT. Coverslips were then mounted with Prolong Gold with DAPI (Invitrogen) and images were captured using a Axioplan 2 fluorescence microscope (Carl Zeiss MicroImaging, Thornwood, NY), fitted with a Hamamatsu ORCA-ER camera (Hamamatsu City, Japan). Mitotic cells, visualized by condensed chromosomal staining with DAPI were counted in 3 fields (20x) and expressed as a percent of total number of cells per field quantified automatically with NIH ImageJ software. LASP1 and DAPI colocalization was evaluated using the colocalization colormap plug-in for ImageJ.

Cloning of the miR-1-133 cluster into a lentiviral vector. pDonr253 is a Gateway Donor vector modified from pDonr201 (Invitrogen). pDonr253 replaces the kanamycin resistance gene with a gene encoding spectinomycin resistance, and contains several sequencing primer sites to aid in sequence verification of Entry clones. The following oligonucleotides (Operon Biotechnologies Inc., Huntsville, AL) were used in this study:

7540: 5′- GGGGACAACTTTGTACAAGAAAGTTGACTCGAGTTTTTGAAATCCTTAAGTCAT CCATAC
7541: 5′- CCTTTTAACACATTACTGCGGATCTTCTTTTCCTTCATGAAATAAAAACCTTAGGG
7542: 5′- CATGAAGGAAAAGAAGATCCGCAGTAATGTGTTAAAAGGAAAAGATTTTTAAACC
7544: 5′- GAGTTTTTGAAATCCTTAAGTCATCCATACATTTTTC
7848: 5′- GGGGACAACTTTGTACAAAAAAGTTGGCGCTAGCAGGATCTAGAAGCAGACTAC
7849: 5′- AGGATCTAGAAGCAGACTACAAAAAAAGAAG

The miR-1(-2)-133a region was amplified from mouse genomic DNA in two forms; a full-length version and a shorter form with a large internal region deleted. The longer form (3960 bp) was made by standard PCR using 200 nM oligos 7847 and 7540. PCR was carried out using Pfusion polymerase (New England Biolabs) under standard conditions using a three minute extension time for 35 cycles. The shorter form was made by overlap PCR in two steps. First, left and right fragments were amplified using primers 7849/7541 and 7542/7544, respectively. The 3' end of the first fragment and 5' end of the second fragment were designed with a 30-bp overlapping sequence. Fragments were amplified for 35 cycles with

a 1-minute extension time, and products were isolated using the QiaQuick PCR purification kit (Qiagen, Valencia, CA). One μl of each overlap PCR product was mixed together in a new PCR reaction with primers 7848 and 7540, and amplified for an additional 25 cycles with a one minute extension time. The final product (1170 bp) was then isolated using the QiaQuick PCR purification kit. The final PCR products contain the miR region flanked on the 5' side with a Gateway attB1 site and on the 3' side a Gateway attB2 site. PCR products were then recombined into pDonr253 using the Gateway BP recombination reaction (Invitrogen) using the manufacturer's protocols. The subsequent entry clones were sequence verified throughout the entire cloned region. Entry clones were subcloned by Gateway LR recombination using the manufacturer's protocols (Invitrogen) into a Gateway-modified version of the lentiviral vector pRRL-CMV-PGK-GFP-WPRE, called Tween, which confers the simultaneous transduction of both reporter GFP and intronic miR region. This vector was constructed by an EcoRV digest of the parental Tween vector, followed by ligation of the Gateway rfa cassette (Invitrogen) to produce a Gateway destination vector. Final expression clones were verified by restriction analysis.

3'UTR reporter construct cloning and luciferase assay. 3' UTR regions from a human prostate tumor cell line were amplified from genomic DNA using PCR. Five UTRs were amplified by standard PCR using 200 nM of each oligo (Operon Biotechnologies Inc., Huntsville, AL) listed in the table below. PCR was carried out using Pfusion polymerase (New England Biolabs) under standard conditions using a 1 minute extension time for 35 cycles. A partial mutant of the *XPO6* UTR was made by incorporating the mutation in a 3' primer and adding additional sequence with an adapter primer. In this case, PCR was carried out for 10 cycles with the initial primers, and then the adapter primer was added and amplification resumed for 30 additional cycles. The *LASP1* UTR mutant was generated by overlap PCR of two halves of the UTR region using the primers listed below. Once the initial products were generated by standard PCR, the products were isolated and used as templates in the subsequence overlap PCR to produce the final clone. In all cases, the final products were isolated using the QiaQuick PCR purification kit (Qiagen, Valencia, CA). The final PCR products contain the UTR region flanked on the 5' side with a Gateway attB1 site and on the 3' side a Gateway attB2 site. The PCR products were recombined into pDonr253 using the Gateway BP recombination reaction (Invitrogen, Carlsbad, CA) using the manufacturer's protocols. pDonr253 is a Gateway Donor vector modified from pDonr201 (Invitrogen). pDonr253 replaces the kanamycin resistance gene with a gene encoding spectinomycin resistance, and contains several sequencing primer sites to aid in sequence verification of Entry clones. The subsequent Entry

clones were sequence verified throughout the entire cloned region. Mutagenesis of all five constructs was carried out using the Quickchange mutagenesis kit (Agilent) using the manufacturer's conditions and the oligos listed in the table below. Final mutant clones were completely sequence verified to ensure their integrity.

Entry clone	Gene 3'UTR	5' oligo	3' oligo	Adapter
7726-E01	*FNI*	6988	6989	
7726-E02	*NOTCH3*	6990	6991	
7726-E03	*PTMA*	6992	6993	
7726-E04	*XPO6*	6994	6995	
7726-E06	*XPO6* partmut	6994	6998	6995

Entry clone	Mutant 3'UTR	5' oligo	3' oligo	Template
7726-E11	*FNI* mutant	7010	7011	7726-E01
7726-E12	*NOTCH3* mutant	7305	7306	7726-E02
7726-E13	*PTMA* mutant	7014	7015	7726-E03
7726-E14	*XPO6* mutant	7016	7017	7726-E06

Oligonucleotides sequences:

6988: 5'-GGGGACAACTTTGTACAAAAAAGTTGGCATCATCTTTCCAATCCAGAGGAAC
6989: 5'-GGGGACAACTTTGTACAAGAAAGTTGACTTAGTCATTTTTATTTCCCTTGCAGGC
6990: 5'-GGGGACAACTTTGTACAAAAAAGTTGGCGACGCTCGTCAGTTCTTAGATCTTGGGGG
6991: 5'-GGGGACAACTTTGTACAAGAAAGTTGAGAGTGTTAACTATTCCTTTATTAGGTGG
6992: 5'-GGGGACAACTTTGTACAAAAAAGTTGGCACAGCAAAAAAGGAAAAGTTAAAC
6993: 5'-GGGGACAACTTTGTACAAGAAAGTTGAGTTAGAACAACTCAGCAAAATAAAATTCCTG
6994: 5'-GGGGACAACTTTGTACAAAAAAGTTGGCGCCTGCTACTGCCTGGGGACACGG
6995: 5'-GGGGACAACTTTGTACAAGAAAGTTGAGGCATTTTATTTCTTTTCATTAAGCTTCTTAG
6996: 5'-GGGGACAACTTTGTACAAAAAAGTTGGCCCAATCTGTACTAATTCTCCAAACCAG
6997: 5'-GGGGACAACTTTGTACAAGAAAGTTGATGGAACAAATCCAAGTAACAACTTTATTGTAG
6998: 5'-CTTTTCATTAAGCTTCTTAGTTTCTTAGTATCACAATGGGAATATGAGAAAACAACAAAAACGTGAGTC
7010: 5'-CAACTGTTTTAATAAAAGATTTCATATCCACAACTTGAAGTTCATC
7011: 5'-GATGAACTTCAAGTTGTGGATATGAAATCTTTTATTAAAACAGTTG
7014: 5'-GACAACAGAAAAACAATCTTATTCCGAGATTCCCAGTAACTTTTTTGTGTATGTAC
7015: 5'-GTACATACACAAAAAAGTTACTGGGAATCTCGGAATAAGATTGTTTTTCTGTTGTC
7016: 5'-GCTCACGACAGTGCCACCTTCTCACATTCCCAGCCAAGGAGAGATGTGACG
7017: 5'-CGTCACATCTCTCCTTGGCTGGGAATGTGAGAAGGTGGCACTGTCGTGAGC
7018: 5'-AAGGTAGTGAATTAATTATTATTCCATTCCCACTATCATGAAGGACTCTGAATAG
7019: 5'-CTATTCAGAGTCCTTCATGATAGTGGGAATGGAATAATAATTAATTCACTACCTT
7020: 5'-CCAATCTGTACTAATTCTCCAAACCAG
7021: 5'-TGGAACAAATCCAAGTAACAACTTTATTG
7022: 5'-GTAAATTTTTGCAGCAAGCAGTCACATATCCACAAACGAACAAACATTATACCTC
7023: 5'-GAGGTATAATGTTTGTTCGTTTGTGGATATGTGACTGCTTGCTGCAAAAATTTAC
7305: 5'-GCAAGGCTATGGAACATGTCCAATCTGGGAATCAGTGAAGTGAGGGAGGTGGGGTGGGG
7306: 5'-CATTTAACTTTAAGAAGGAGATATATACCATGGAAAAGGCAAAAAAAAGTGTGGAGATTC
8755: 5'-GGGGACAACTTTGTACAAAAAAGTTGGCACCCGCAGCGCCCCCATCTGTCTTCAGC
8756: 5'-GGGGACAACTTTGTACAAGAAAGTTGATCCGCAGGTAAAAATTATACTTTTATTTGAG
8757: 5'-GCGCCCCCATCTGTCTTCAGCTTCAACCACGGCATCGCATCCGTCCTGGGCGTGAC
8758: 5'-GGGTCCTGGCAGTCAGGCTCACCCCAGCCCTGGTTGAAGTGGGTATGTGAGGAGCTGGGC

8759: 5′-GGGGTGAGCCTGACTGCCAGGACCCCAGGTCAGGGGCTCCCTTTCAACCCCAGAGTGGGATCCACTTCTTGG
8760: 5′-TCCGCAGGTAAAAATTATACTTTTATTTGAGTCACCAGGAGAAAG

To produce the final constructs entry clones were subcloned by Gateway LR recombination using the manufacturer's protocols (Invitrogen, Carlsbad, CA) into a Gateway-modified version of the psiCHECK2 expression vector which contains both luciferase and renilla genes and uses renilla as the reporter gene. This Gateway-modified destination vector was constructed by an EcoRV digest of the parental vector, followed by ligation of the Gateway rfa cassette (Invitrogen, Carlsbad, CA).